

Supercritical N₂ Processing as a Route to the Clean Dehydrogenation of Porous Mg(BH₄)₂

Supporting Information

Nicholas P. Stadie*¹, Elsa Callini¹, Bo Richter², Torben R. Jensen², Andreas Borgschulte¹,
and Andreas Züttel¹

¹ Empa, Swiss Federal Laboratories for Materials Science and Technology, Dübendorf, Switzerland

² Department of Chemistry, Aarhus University, Aarhus, Denmark

*E-mail address: nicholas.stadie@empa.ch

I. Introduction

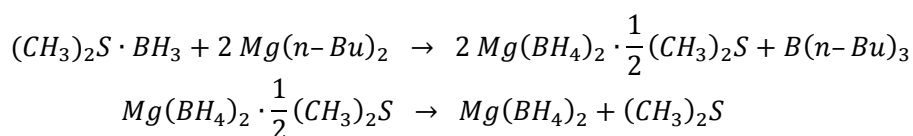
Materials characterization techniques, including X-ray diffraction (XRD), attenuated total reflectance infrared spectroscopy (ATR-IR), nitrogen gas adsorption, and temperature-program decomposition coupled with infrared spectroscopy (TPDIR) were performed to support the conclusions reported in “Supercritical N₂ Processing as a Route to the Clean Dehydrogenation of Porous Mg(BH₄)₂.” The experimental details of these measurements and analyses, as well as those of the materials synthesis and the supercritical drying (ScD) treatments are given below.

The primary conclusion of our studies is that by employing an appropriate technique for eliminating guest impurities in the porous structure of γ -Mg(BH₄)₂ via supercritical nitrogen drying (NScD), the material desorbs hydrogen cleanly under heating. The lack of diborane among the thermodynamic decomposition products of Mg(BH₄)₂ confirms its description as a stable borohydride and assists to elucidate the role of diborane in the decomposition reactions of borohydride materials as a whole. In other words, the presence of diborane in the gaseous decomposition products of complex hydride materials can be due to either its relevance to the reaction mechanism of decomposition or its preexistence in the pores or on the surface of the material (as a result of synthesis or preparation). The latter is an especially important consideration for high surface area hydrides such as γ -Mg(BH₄)₂. This study establishes ScD treatments, especially those employing nitrogen as the supercritical fluid (NScD treatments), as highly effective and important techniques toward increasing the hydrogen purity and storage capacity of reactive, porous materials.

An overview of the materials synthesis and supercritical drying techniques used in this study is given in sections II-III. The central measurements presented in this study, employing a combination of gravimetric and spectroscopic techniques (TPDIR), allowed the quantification of total mass loss and the specific mass loss associated with each gas species evolved during decomposition. The details of this technique and the analysis of its results are given in sections IV-V. X-ray diffraction studies and nitrogen adsorption measurements of the materials before and after NScD treatment are presented in sections VI-VII to ascertain whether NScD treatments have an effect on the crystal structure or surface/porosity characteristics of γ -Mg(BH₄)₂. ATR-IR spectra of the untreated and NScD-treated samples are shown in section VIII.

II. Materials Synthesis

The γ -Mg(BH₄)₂ investigated in this study was obtained by wet chemical synthesis, from borane dimethylsulfide and di-*n*-butylmagnesium via the following (unbalanced) reaction:



Typically 10 mL Mg(*n*-Bu)₂ (1.0 M solution in heptanes) was added to 18 mL of (CH₃)₂S·BH₃ (2.0 M solution in toluene) as previously described.¹¹ The intermediate, Mg(BH₄)₂·½ (CH₃)₂S (~0.7 g), was dried in vacuo at room temperature for 1-2 h. The final product was obtained by further drying in vacuo at 80°C and 2 × 10⁻² mbar for 12-16 h, yielding ~0.45 g pure γ -Mg(BH₄)₂. This sample is hereafter referred to as “untreated.”

III. Supercritical Drying Treatment

In this study, samples of γ -Mg(BH₄)₂ were treated with both supercritical CO₂ and supercritical N₂ drying methods referred to as CScD and NScD, respectively. In both cases, the same basic procedure was applied, except that the temperatures and pressures were adjusted to account for the different critical points of the two fluids. The phase diagrams of CO₂ and N₂, calculated from the modified Benedict-Webb-Rubin equation of state (implemented by Refprop²³), are shown in Figure S1. The critical point of CO₂ is higher than N₂, allowing for supercritical fluid treatments at near ambient temperature and modestly high pressure. While supercritical N₂ can also be achieved under such conditions, to reach a high density (liquid-like) supercritical state capable of high solvent ability, low temperatures must be used. For NScD treatments, a low temperature isothermal bath was maintained by the use of a furnace submersed in liquid nitrogen, tunable between 80-298 K (see Figure S2).

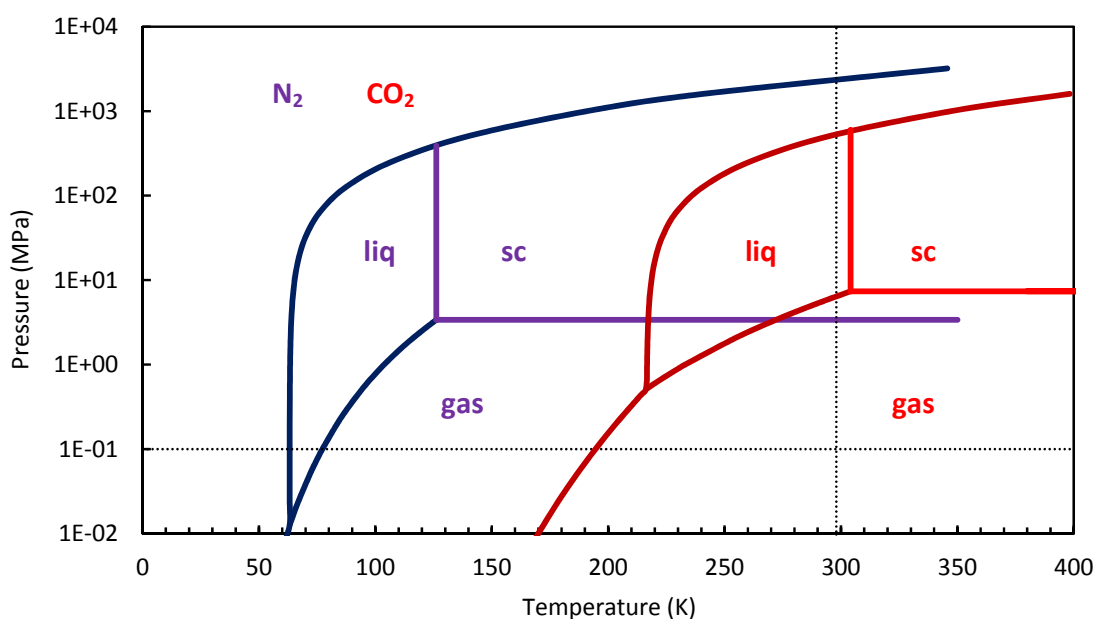


Figure S1. Pressure-temperature phase diagram of CO₂ (red) and N₂ (purple), from the modified Benedict-Webb-Rubin equation of state. Ambient temperature and pressure are shown as dotted lines.

For ScD treatments, a simple custom-built gas dosing apparatus was used (see Figure S3). It is constructed of stainless steel SITEC components and is suitable for containing gas pressures between 0.01 Pa (10⁻⁴ mbar) and 30 MPa. It is equipped with a Pirani vacuum sensor (VSP62M, Thyracont Vacuum Instruments GmbH), two high pressure sensors for 0-1 and 0-30 MPa ranges (PA(A)-33 X, Keller AG), and K-type thermocouples (Omega Engineering Inc.). The sample holder can be placed inside one of two custom-built cylindrical furnaces: one for high temperatures (0-500°C) and one for immersion in a liquid N₂ Dewar for low temperatures (80-298 K). The temperature program is set by a multichannel process controller (Imago 500, Jumo GmbH) and all sensors are monitored by a custom Labview interface. The bulk of the apparatus is maintained at a constant temperature of 40°C (all parts excluding the sample holder and dip tube). Carbon dioxide (99.998%) and nitrogen (99.999%) gases were obtained from Messer AG, Schweiz, and held at room temperature and ~10 MPa. The apparatus was evacuated and purged with the fluid of choice numerous times before each drying procedure to maintain gas purity.

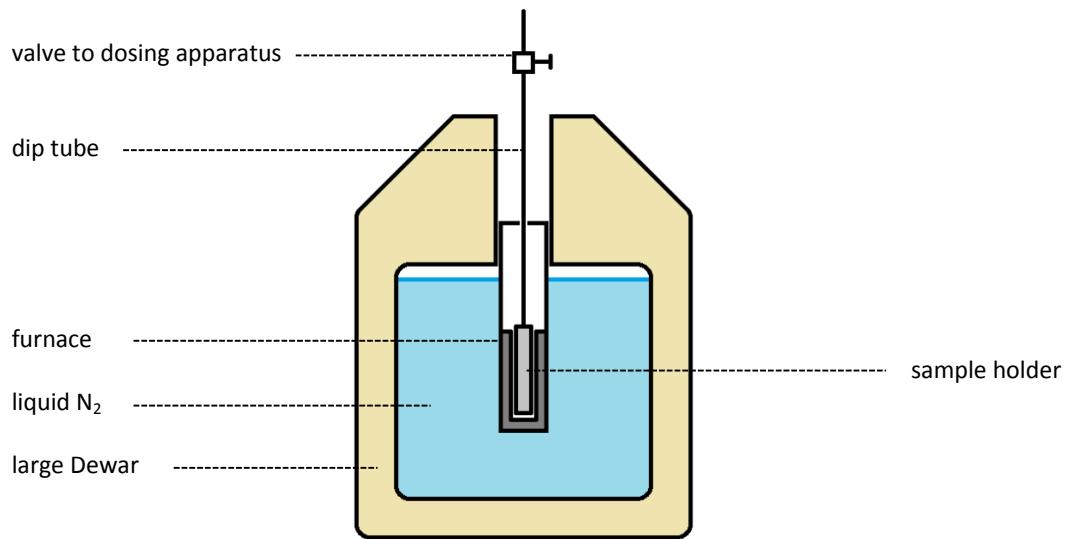


Figure S2. Schematic depiction of the cryostatic furnace used to maintain low temperatures (110-150 K) for NScD treatments.

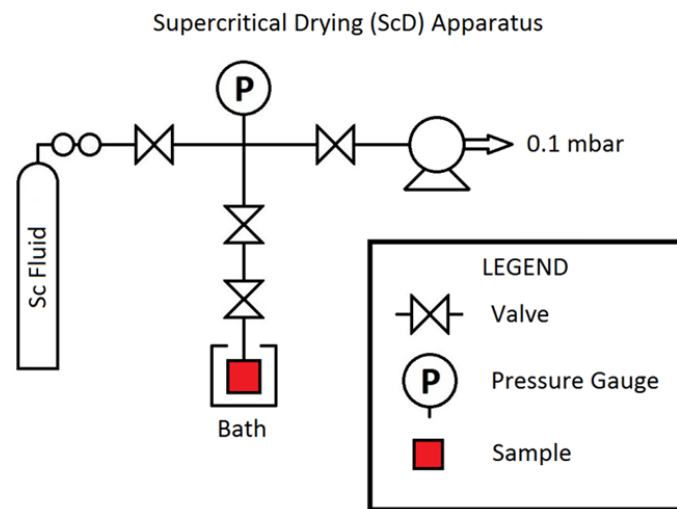


Figure S3. Schematic depiction of the custom built ScD apparatus used for NScD and CScD treatments. The isothermal bath surrounding the sample was either an ice water bath, a high temperature furnace, or the cryostatic furnace shown in Figure S2.

Carbon dioxide supercritical fluid drying (CScD) treatments were typically performed on 0.2 g of γ -Mg(BH₄)₂, with the following procedure:

1. Inside a glovebox (Ar atmosphere, <0.1 ppm H₂O/O₂), place 0.2 g of sample into sample holder (Swagelok 6 mm tubing blank, 0.5 mm inner diameter) and tighten with compression fitting to stainless steel dip tube with valve. Close valve and remove sample holder from glovebox.
2. Attach sample holder, valve, and dip tube to ScD dosing apparatus.
3. Evacuate the apparatus and subsequently the sample holder (at room temperature) to <0.1 Pa for 30 min.
4. Immerse sample holder and a thermocouple in an ice water bath (0°C) and continue to evacuate for 10 min.
5. Fill the apparatus and sample holder volumes with CO₂ up to 7 MPa (gas over liquid). Allow to equilibrate for 30 min.
6. Soak the sample in liquid CO₂ for 4 h and maintain the ice bath.
7. Remove the ice bath and place the sample holder into a cylindrical furnace. Heat the sample holder to 40°C with a temperature ramp of 1°C per min. Vent the gas pressure when it reaches 9 MPa and maintain.
8. Soak the sample in supercritical CO₂ for 1 h.
9. Degas the apparatus and sample holder at 40°C to vacuum pressure slowly over 12-20 h.
10. Remove the sample holder from the furnace and continue to evacuate the sample holder to <0.1 Pa for 30 min.
11. Close valve between sample and apparatus, and remove the sample holder. Open the sample holder inside a glovebox (Ar atmosphere, <0.1 ppm H₂O/O₂) and remove the treated sample.

Nitrogen supercritical fluid drying (NScD) treatments were typically performed on 0.2 g of γ -Mg(BH₄)₂, with the following procedure:

1. Inside a glovebox (Ar atmosphere, <0.1 ppm H₂O/O₂), place 0.2 g of sample into sample holder (Swagelok 6 mm tubing blank, 0.5 mm inner diameter) and tighten with compression fitting to stainless steel dip tube with valve. Close valve and remove sample holder from glovebox.
2. Attach sample holder, valve, and dip tube to ScD dosing apparatus.
3. Evacuate the apparatus and subsequently the sample holder (at room temperature) to <0.1 Pa for 30 min.
4. Place the sample holder and a thermocouple into the cryostatic furnace (shown in Figure S2) and cool to 110 K. Equilibrate and continue to evacuate for 30 min.
5. Fill the apparatus and sample holder volumes with N₂ up to 2 MPa (gas over liquid). Allow to equilibrate for 30 min.
6. Soak the sample in liquid N₂ for 4 h at 110 K and 2 MPa.
7. Heat the furnace to 150 K with a temperature ramp of 2 K per min. Vent the gas pressure when it reaches 7 MPa and maintain.
8. Soak the sample in supercritical N₂ for 1 h.
9. Degas the apparatus and sample holder at 150 K to vacuum pressure slowly over 12-20 h.
10. Remove the sample holder from the furnace and continue to evacuate the sample holder to <0.1 Pa for 60 min at room temperature.
11. If iterated treatments are desired, repeat steps 4-10.
12. Close valve between sample and apparatus, and remove the sample holder. Open the sample holder inside a glovebox (Ar atmosphere, <0.1 ppm H₂O/O₂) and remove the treated sample.

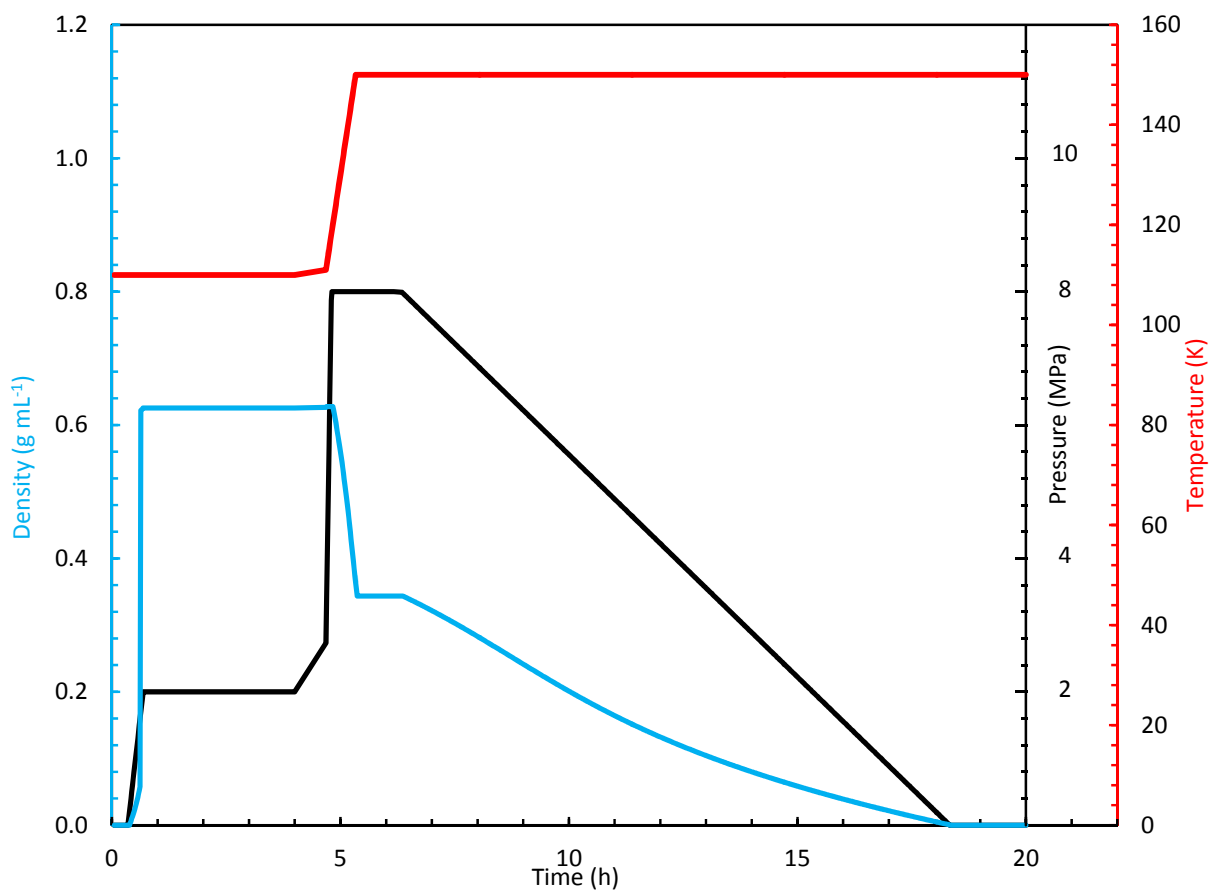
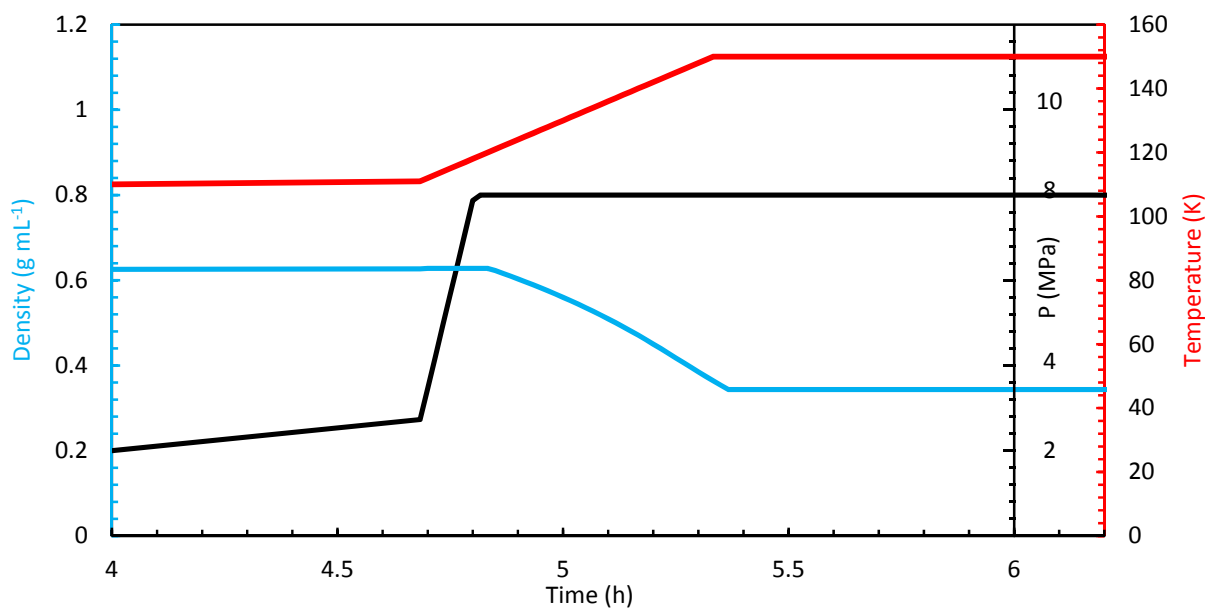


Figure S4. The density of fluid N_2 as a function of pressure and temperature during a typical NScD treatment: the entire experiment (above) and a detailed region (below). The detail during heating to the supercritical state is shown (below) to emphasize the smooth density change characteristic of this step.



The density of nitrogen in the sample holder as a function of time throughout a typical NScD experiment used in this study is shown in Figure S4. A key feature of the methodology described herein is to achieve very high fluid density during the liquid/supercritical soak phases (step 6), in this case reaching $>0.6 \text{ g mL}^{-1}$ ($\sim 12 \text{ mol L}^{-1}$). This value is comparable to those obtained during typical supercritical CO_2 drying experiments, e.g. 18 mol L^{-1} ,¹⁷ though at the much lower temperatures characteristic of N_2 . The decrease in fluid density that occurs during heating into the supercritical state is merely due to the decision to prevent the pressure from increasing beyond 8 MPa. This would certainly not need to be the case if higher pressure apparatus were used: e.g. supercritical N_2 solvent densities of $\sim 20 \text{ mol L}^{-1}$ are readily achievable at 150 K and 20 MPa. The smooth transition in density from the liquid to the supercritical state to the gas state between 5-20 h (corresponding to step 9) is the second important feature of this methodology, and leads to the successful removal of impurity species (especially diborane in the case of $\gamma\text{-Mg}(\text{BH}_4)_2$).

The solvent power of supercritical N_2 with respect to commonly encounter molecular solutes has not been well reported in the literature at these densities. However, the results of this study indicate N_2 is indeed an effective solvent of both diborane and a species resembling *n*-butane (the “*n*-butyl” impurity, see section V), though requiring typically 3 iterations of the above treatment to achieve a final product with $<0.2 \text{ mass\%}$ impurities.

IV. Temperature-Program Decomposition with Infrared Spectroscopy (TPDIR)

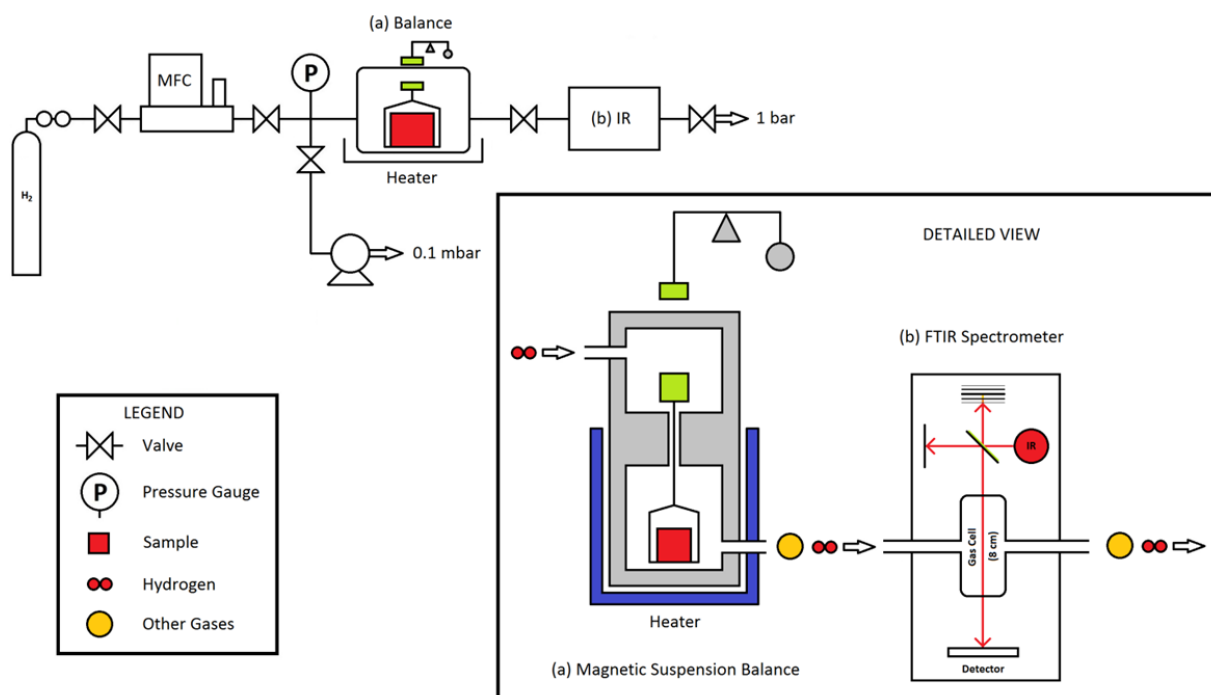


Figure S5. Schematic depiction of the TPDIR apparatus where the flow of H_2 (red circles) is shown to pass from the mass flow controller (MFC) through the magnetic suspension balance (a) from where it carries gaseous decomposition products or impurities (yellow circles) to the FTIR spectrometer (b) and out to exhaust.

The principle measurements performed in this study follow a technique combining gravimetry with gas phase infrared spectroscopy, as previously described.¹² To investigate the decomposition of a material under heating, it is placed in an open crucible under H₂ flow (which carries gas phase products to the downstream spectrometer cell) and heated from room temperature to a setpoint under a given ramp program; hence, the method is herein called temperature-program decomposition with infrared spectroscopy (TPDIR).

The total weight change of the solid (and possibly liquid) reactants/products during heating is measured using a magnetic suspension balance (IsoSORP E10, Rubotherm GmbH) with a resolution of 0.01 mg (maximum sample weight is 25 g). The sample lies in an open bucket (crucible) which hangs inside a cylindrical pressure cell that is further held at a constant temperature by an external furnace. The sample environment can be evacuated to <10⁻³ mbar or pressurized up to 10 MPa. The mass change of the sample is derived by taking into account the effects of buoyancy under the specific conditions inside the balance, using the modified Benedict-Webb-Rubin equation of state (implemented by Refprop²³). The balance head is kept at a constant temperature of 25°C by an external water circulation system to reduce errors from temperature gradients in the balance. The balance is coupled to a glovebox for sample loading under an inert argon environment.

The balance is used in open-flow format, where the inlet and outlet valves to the pressure cell are open. Hydrogen gas (99.999%, from Messer AG) flow into the balance is controlled by a mass-flow controller (1259C, MKS Instruments Inc.) in combination with a custom Labview interface. The outflow is into ambient pressure (to fume hood exhaust) via an infrared spectrometer gas cell (Alpha FT-IR, Bruker Corp.). The gas cell is 8 cm in length and the spectrometer has a resolution of 0.9 cm⁻¹. The scan program, spectrum averaging, and background correction were performed by OPUS software in combination with a custom Labview interface.

The complete TPDIR experimental apparatus is shown schematically in Figure S5. Before experiments, the system was evacuated to <10⁻³ mbar for 30 min and then purged with flowing H₂ (500 mL min⁻¹) for 60 min. Measurements of the empty sample holder were performed to deduce the instrumental error from temperature gradients in the balance (~5.4 × 10⁻⁷ g K⁻¹ to first order). Measurements of high surface hydride materials under H₂ flow, even at extremely high purity (99.999%), were found to result in some mass accumulation as a function of flow volume (~1.3 × 10⁻⁹ g mL⁻¹ for γ-Mg(BH₄)₂ at 298 K, which corresponds to ~10 ppm H₂O and/or trace other gases as specified by the gas supplier), and these effects were also corrected. In summary, to calculate the total mass change of the solid reactants/products of decomposition during heating, the corrections employed were: buoyancy, temperature effects, and flow mass accumulation.

The following standard TPDIR experiment was performed for each sample in this study:

1. Load the sample in the balance and weigh in argon atmosphere at room temperature.
2. Install the pressure-temperature cell around the sample, and evacuate the entire gas manifold to <10⁻³ mbar for 30 min at room temperature. Close the manifold to vacuum.
3. Begin the hydrogen gas flow from the bottle into the closed balance chamber up to ~2 bar, then throttle the flow into the IR gas cell which is initially at ambient pressure. The gas flows out of the spectrometer cell and into exhaust, equilibrating at 1 bar. Purge the entire system at a flow rate of 500 mL min⁻¹ for 30-60 mins (until the IR background is featureless).
4. Reduce the flow to 200 mL min⁻¹ at 1 bar for the remainder of the experiment.
5. Collect the background IR spectrum (16 scans), for subtraction from all subsequent spectra.

6. Start the automatic IR scan program: 16 scans per spectrum, 1 spectrum per 1.5 min, and scan range of 4500-1000 cm^{-1} at a resolution of 0.9 cm^{-1} .
7. Start the balance (and heating) program with 4 segments: hold at room temperature (for equilibration and to quantify errors) for 1 h, heat to 593 K at 2 K min^{-1} , hold at 593 K for 5 h, and finally cool to room temperature.
8. Stop the flow and collect the solid decomposition products. Store the products under argon atmosphere or remove for further characterization.

The samples measured in this study were: un-, CScD-, 1x NScD-, and 3x NScD-treated $\gamma\text{-Mg}(\text{BH}_4)_2$.

V. Identification of Decomposition Products and Impurities

The gaseous components of the downstream flow during TPDIR experiments were identified by comparison of the measured IR spectra to the NIST database²⁴ or to internal reference spectra. The following gases were screened: water, carbon dioxide, carbon monoxide, diborane, boron trifluoride, hydrogen chloride, methane, methanol, methyl formate, and various solvents (e.g. dimethyl sulfoxide (DMSO), dimethyl sulfide (DMS), 1,4-epoxybutane (tetrahydrofuran, THF), methylbenzene (toluene), *n*-butane, *n*-hexane, and *n*-heptane). It should be noted that while the calibrated NIST data (those containing information as to the spectrometer cell length and concentration of gas used) are often not of high resolution (typically 4 cm^{-1}), they allow for reasonably accurate screening of a large number of gas species for later quantification. The NIST references were compared when possible with internal reference IR spectra (e.g. THF and water) and the results were in acceptable agreement.

In most cases, prominent features could be identified for each gas species detected, making identification and indexing of the spectral features unambiguous. For example, the IR spectra collected at 400 K during TPDIR experiments of the four samples shown in Figure 1 of the main text are shown in detail in Figures S6 and S7 below. In exception, the broad C-H stretching mode detected at $\sim 2900 \text{ cm}^{-1}$ in almost all the samples studied was typically not distinct enough to be unambiguously identified. We refer to this species as an “*n*-butyl” impurity, a molecule or complex that is leftover from wet chemical synthesis (for synthesis details, see section II). The following is an explanation of this nomenclature. The α - and γ -phases of $\text{Mg}(\text{BH}_4)_2$ (and hence the β -phase as well) are typically prepared in a solvent containing such species as THF, DMS(O), *n*-butyl compounds, heptanes, and toluene. All of these species exhibit a prominent C-H stretching feature at 2800-3100 cm^{-1} , which is characteristic of alkyl-containing compounds. The presence of the aromatic C-H stretch in toluene between 3100-3000 cm^{-1} allows easy identification or elimination of it compared to the non-aromatic compounds; we did not detect any toluene in the decomposition of samples in this study. Secondly, the prominent features found at 1500-1000 cm^{-1} characteristic of DMSO and DMS allow easy identification of these species when compared to the others; likewise, none were detected in this study. We therefore conclude that the C-H stretching band between 3010-2810 cm^{-1} must be from an alkane-containing precursor or intermediate: di-*n*-butylmagnesium, tri-*n*-butylborane, *n*-butane, or heptanes, or possibly THF. While we cannot rule out the possibility of heptanes residing in $\gamma\text{-Mg}(\text{BH}_4)_2$ after synthesis (THF was not used in the preparation of the γ -phase), we refer to this unidentified species as “*n*-butyl” due to the high probability it is the case.

The mass of the “*n*-butyl” impurity species was taken to be 58 g mol^{-1} and its quantification was performed in comparison to the infrared spectrum of *n*-butane. In this way, the mass loss calculated from “*n*-butyl” impurities was found to be consistent with the total mass loss measured in the balance over the course of TPDIR experiments (see Figure 3B of the main text), which further justifies the choice of name for this species.

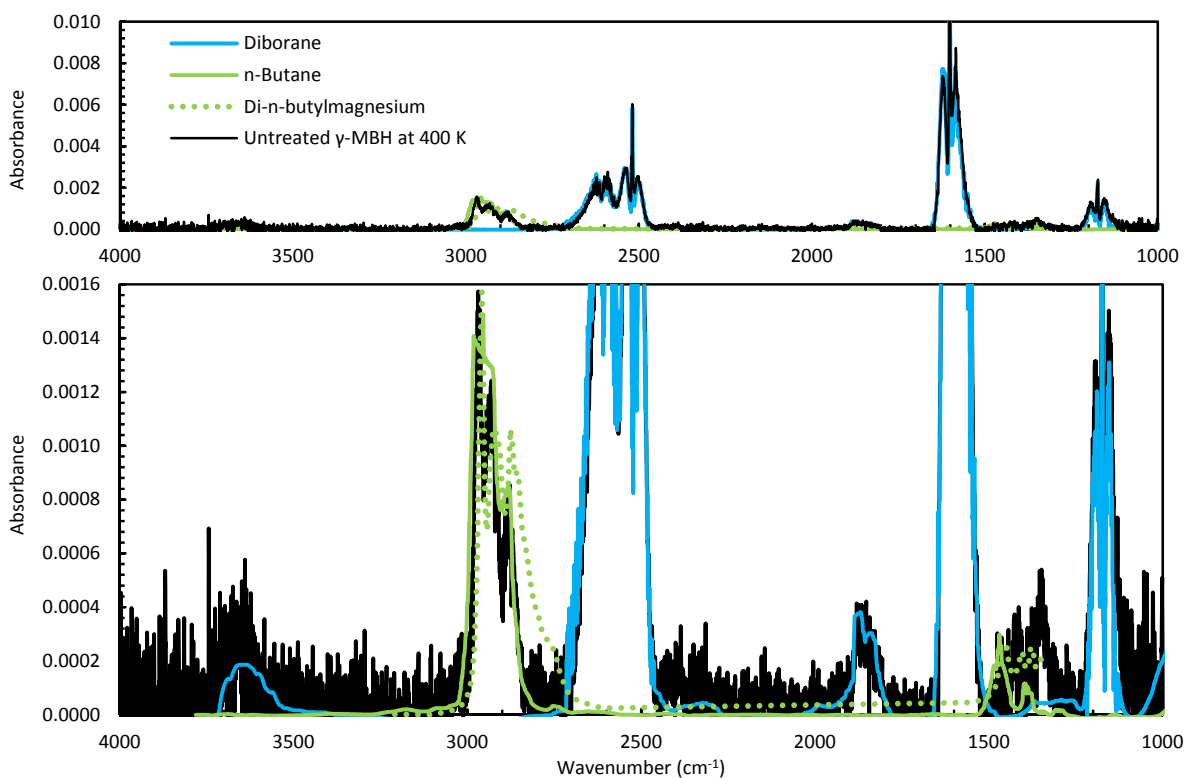
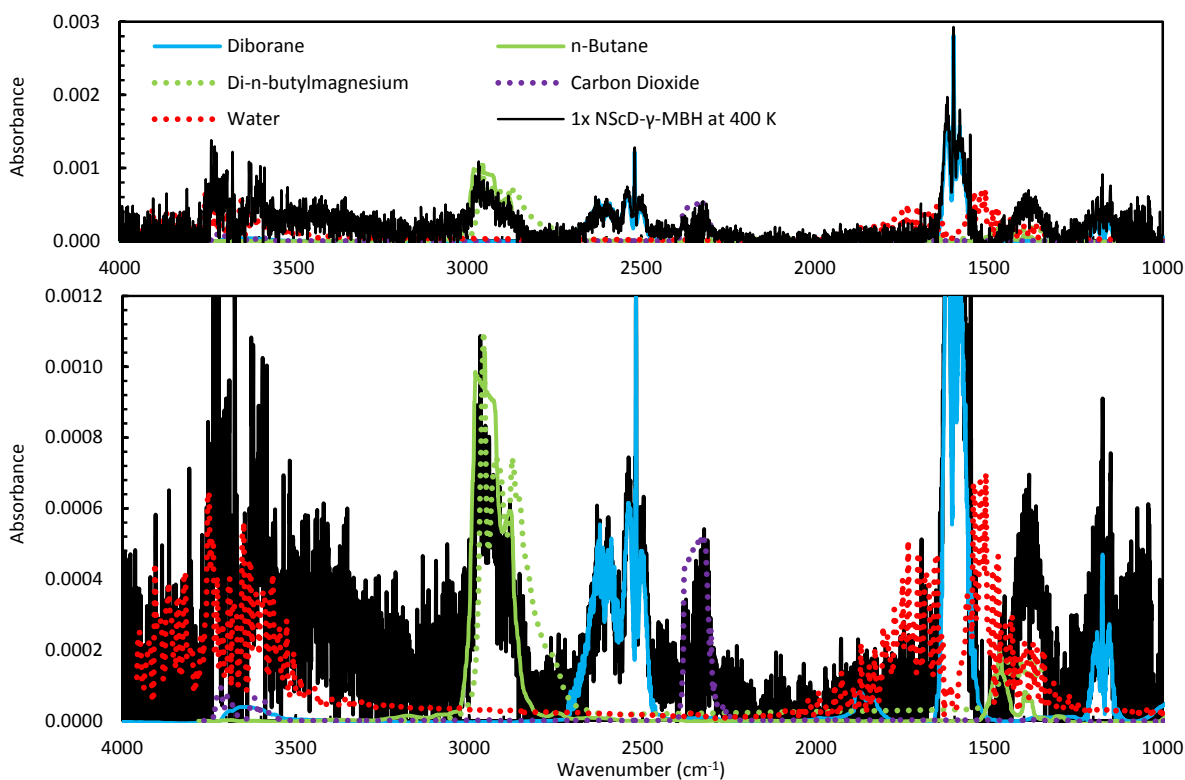


Figure S6A. IR spectra of the gas phase emitted from untreated $\gamma\text{-Mg}(\text{BH}_4)_2$ (above) and 1x NScD-treated $\gamma\text{-Mg}(\text{BH}_4)_2$ (below) during heating. The spectra were measured at 400 K during a 2 K min^{-1} ramp. The components of the gas are identified and quantified, including trace impurities like H_2O and CO_2 .



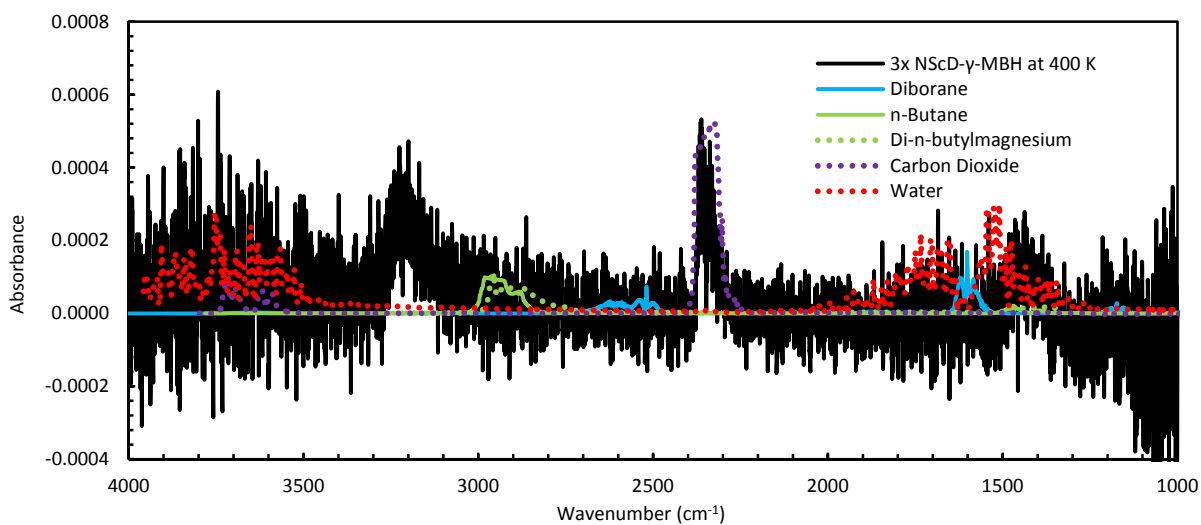
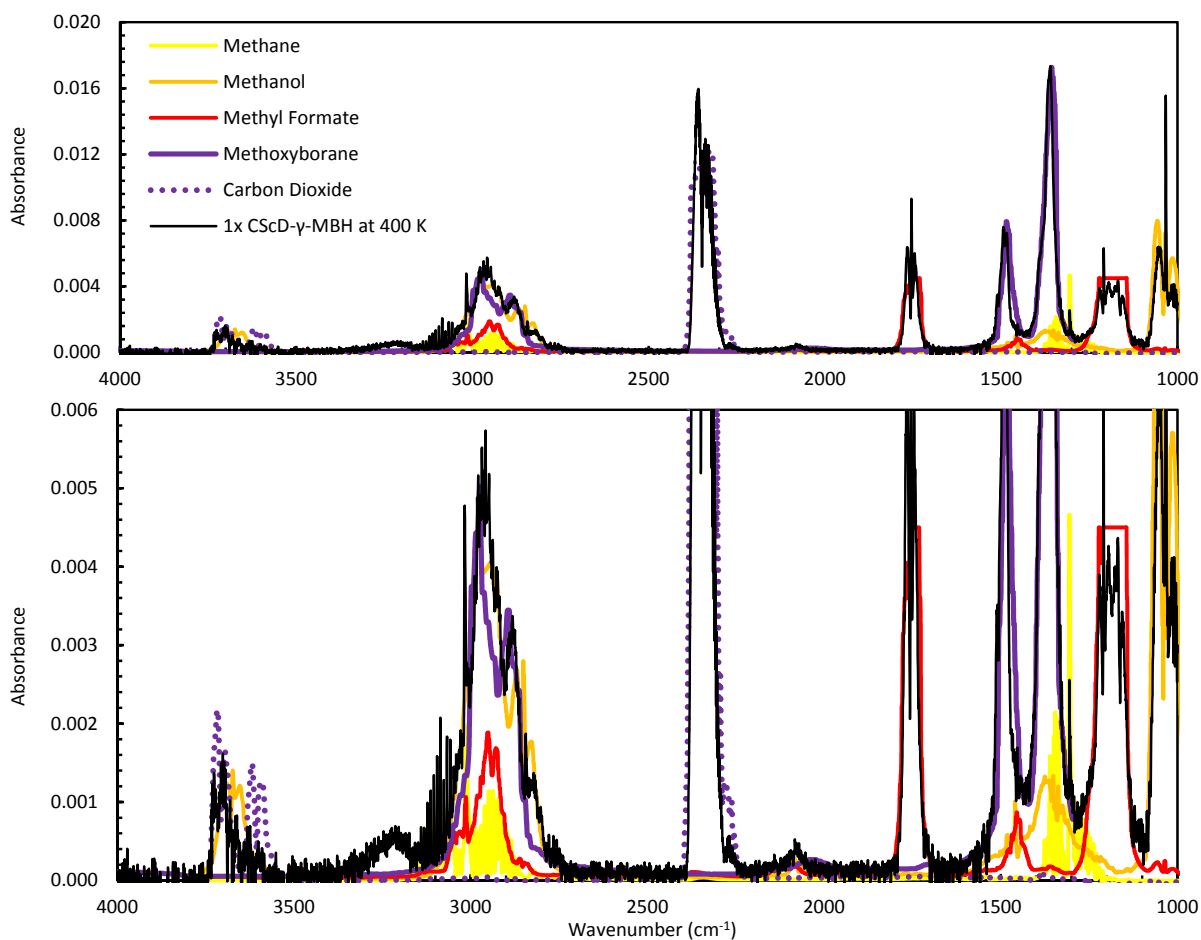


Figure S6B. IR spectra of the gas phase emitted from 3x NScD-treated γ -Mg(BH₄)₂ (above) and 1x CScD-treated γ -Mg(BH₄)₂ (below) during heating. The spectra were measured at 400 K during a 2 K min⁻¹ ramp. The components of the gas in the 3x NScD-treated sample (above) were not easily identified since their features were at or below the limits of the instrument (though trace CO₂ and H₂O were detected).



The concentration of all screened components of the gas mixture (where the bulk is flowing H₂) as a function of temperature throughout TPDIR experiments is plotted in Figures S7A-C, corresponding to untreated, NScD-treated, and CScD-treated samples respectively.

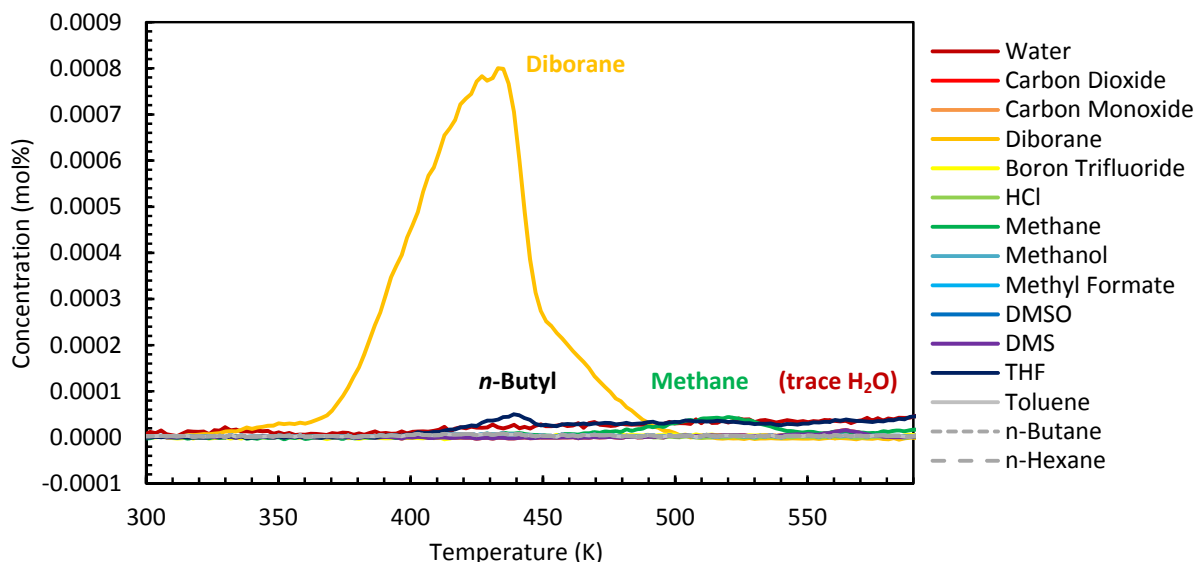


Figure S7A. Quantification of all screened gases as a function of temperature during heating of untreated γ -Mg(BH₄)₂ between 298-593 K under flowing H₂ (0.1 MPa, 200 mL min⁻¹). Sample size: 0.26344 g.

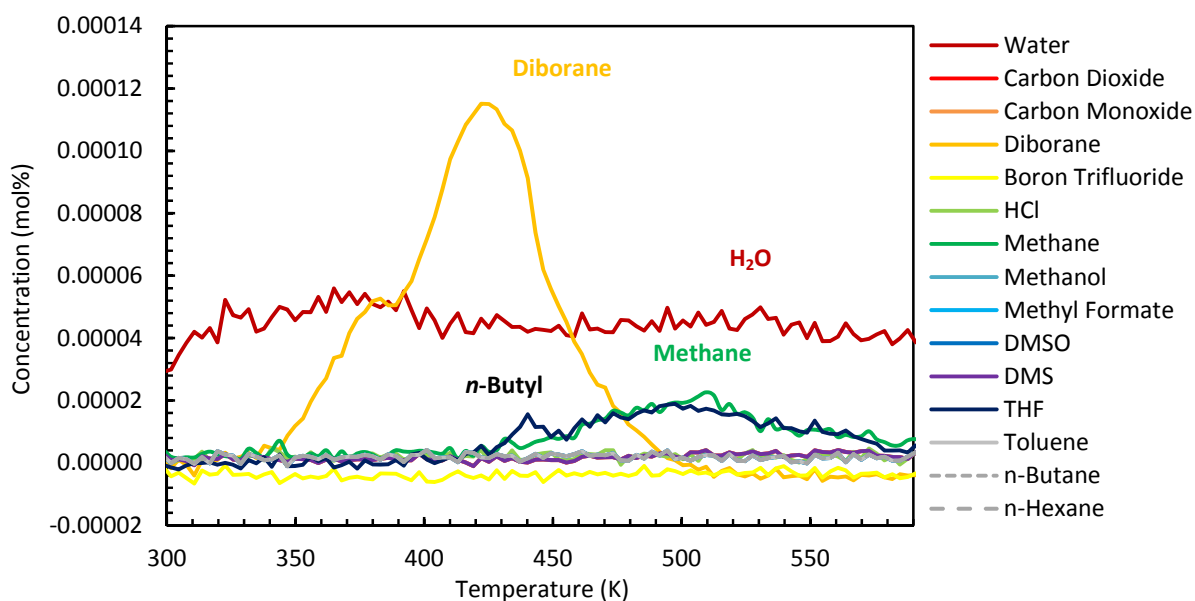


Figure S7B. Quantification of all screened gases as a function of temperature during heating of NScD-treated (1x) γ -Mg(BH₄)₂ between 298-593 K under flowing H₂ (0.1 MPa, 200 mL min⁻¹). Sample size: 0.25442 g.

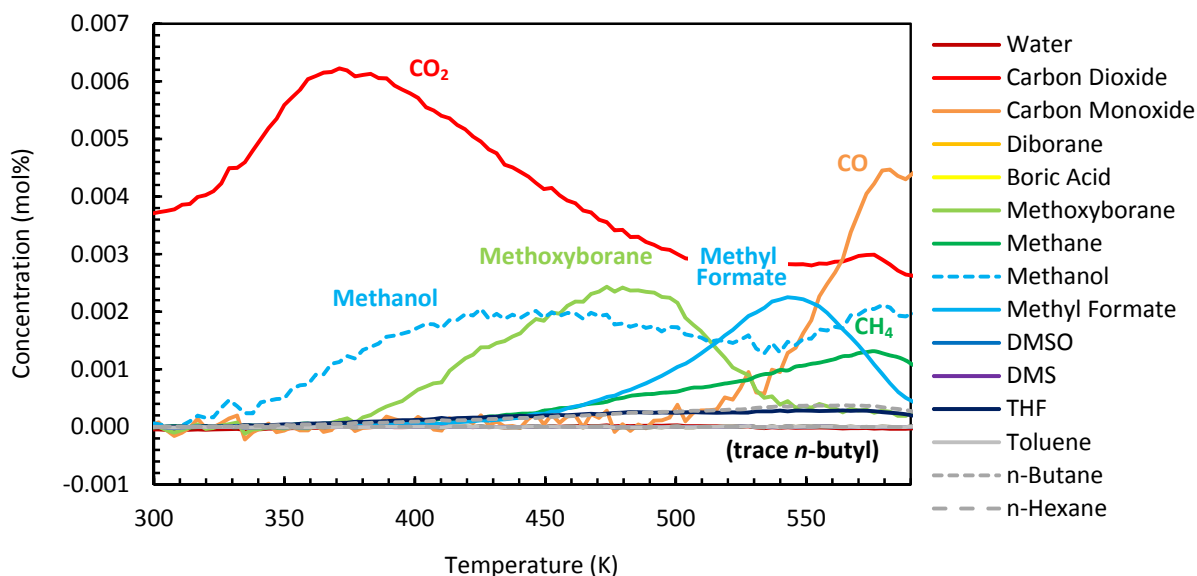


Figure S7C. Quantification of all screened gases as a function of temperature during heating of CScD-treated γ - $\text{Mg}(\text{BH}_4)_2$ between 298-593 K under flowing H_2 (0.1 MPa, 200 mL min^{-1}). Sample size: 0.13361 g.

The large number of coincident species that evolved upon decomposition of the CScD-treated γ - $\text{Mg}(\text{BH}_4)_2$ (e.g. see Figure S6B bottom) made the specific assignment of the IR bands a challenge. This was compounded by the lack of a NIST (or other) IR reference for pure methoxyborane, the major reaction product of methanol and diborane at elevated temperatures.²⁵ However, the B=O stretch at $\sim 1358 \text{ cm}^{-1}$ and its uniquely large $\text{B}^{10}\text{-B}^{11}$ isotopic shift (due to the heavy oxygen atom) were identifiable and upon comparison of the spectrum to the expected bands of methoxyborane, a specific match was confirmed. An approximate IR spectrum for methoxyborane was used as a reference for analysis based on a subtraction of the spectrum obtained for all the reaction products of diborane and methanol at 573 K²⁵ by the individual spectra for boroxin, methane, and dimethyl ether (leaving only methoxyborane).

The decomposition of CScD-treated γ - $\text{Mg}(\text{BH}_4)_2$ resulted in the evolution of the following series of gases as a function of temperature and time: carbon dioxide, methanol, methoxyborane, methyl formate, methane, and carbon monoxide. These are evidently the gaseous products of the reaction between $\text{Mg}(\text{BH}_4)_2$ and CO_2 , and the subsequent reactions between these gases themselves, analogous to those observed upon the reaction of CO_2 with LiAlH_4 .¹⁹ Perhaps surprisingly, the appearance of methane and methanol is in a different order from that observed for LiAlH_4 (with methanol evolving before methane in this case), though the comparability of these studies is certainly questionable (one being performed in flowing gaseous CO_2 and one being performed ~ 1 -2 h after exposure to supercritical CO_2 for 24 h). In addition, it has long been known that the gas solid reactions of CO_2 with borohydrides and alanates are a matter of considerable complexity; e.g. there seem to be no easily recognizable patterns even between the reaction mechanisms of CO_2 with NaBH_4 and LiBH_4 .²⁶

VI. X-Ray Diffraction

X-ray diffraction (XRD) patterns were measured at room temperature using a Bruker D8 diffractometer and Cu $K\alpha_{1,2}$ radiation. The diffractometer is equipped with a Goebel mirror and a linear detector system (Vantec). Samples for XRD measurements were prepared by filling into glass capillaries (0.5 mm inner diameter, 0.1 mm wall thickness) and sealed under argon atmosphere in a glovebox. The raw patterns were treated by removing the amorphous background due to the rotating capillary.

Measurements of the untreated γ -Mg(BH₄)₂ and NScD-treated γ -Mg(BH₄)₂ are shown in Figure S8. The peaks were indexed based on the previously reported structure¹¹ of γ -Mg(BH₄)₂ and no peaks belonging to the α - or β -phases were detected. It can be seen that both samples are highly crystalline and NScD treatments do not have a damaging effect on the crystallinity or the phase purity of the material. A diffraction pattern of untreated Mg(BH₄)₂ purchased from Sigma Aldrich is also shown, identifying this commercial material as γ -Mg(BH₄)₂ as well (though the phase is not specified nor guaranteed by the supplier, and may vary from batch to batch). Rietveld refinement analysis of the patterns before and after NScD treatment did not show any changes to the crystal structure.

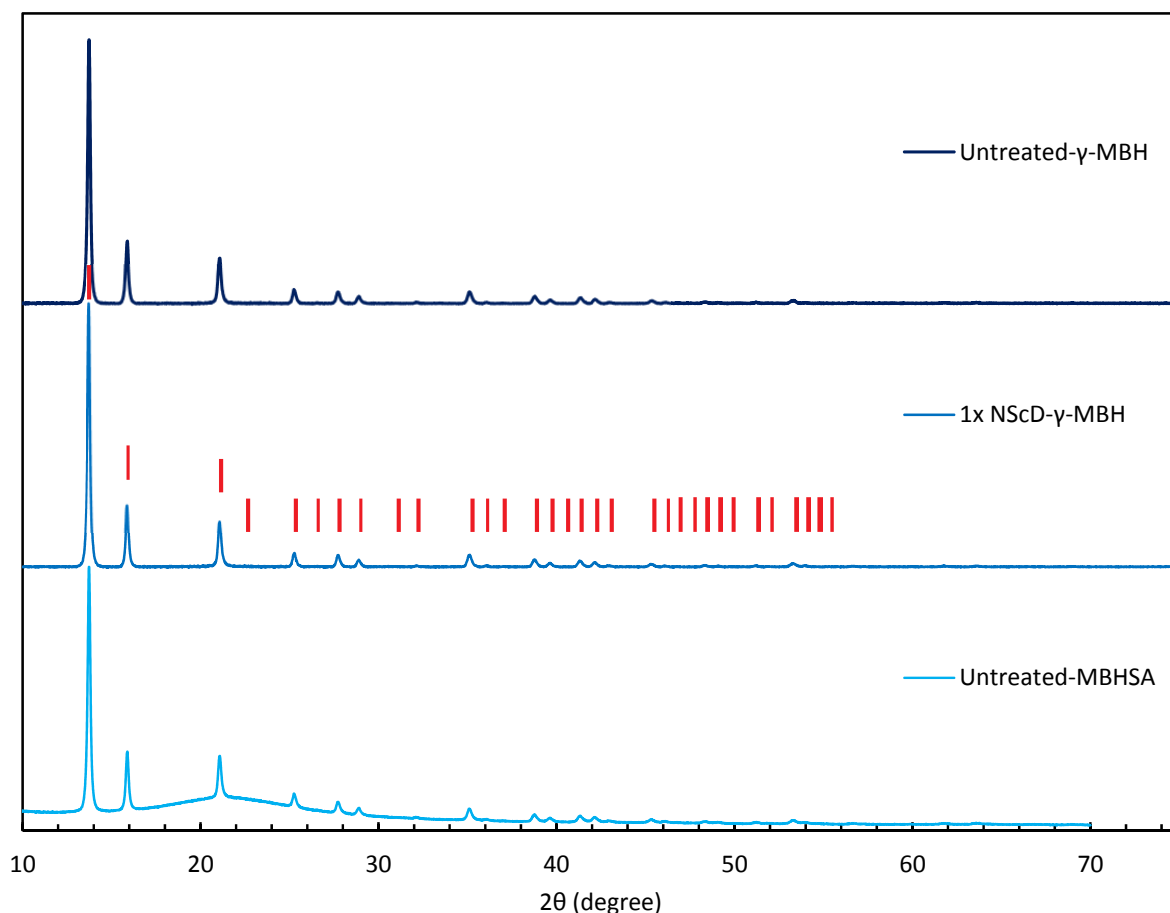


Figure S8. Normalized XRD patterns of γ -Mg(BH₄)₂: untreated (top) and after 1x NScD treatment (middle). All peaks identified correspond to pure γ -Mg(BH₄)₂,¹¹ indicated in red. The normalized XRD pattern of untreated Mg(BH₄)₂ received from Sigma Aldrich (“MBHSA”, bottom) is also shown for reference.

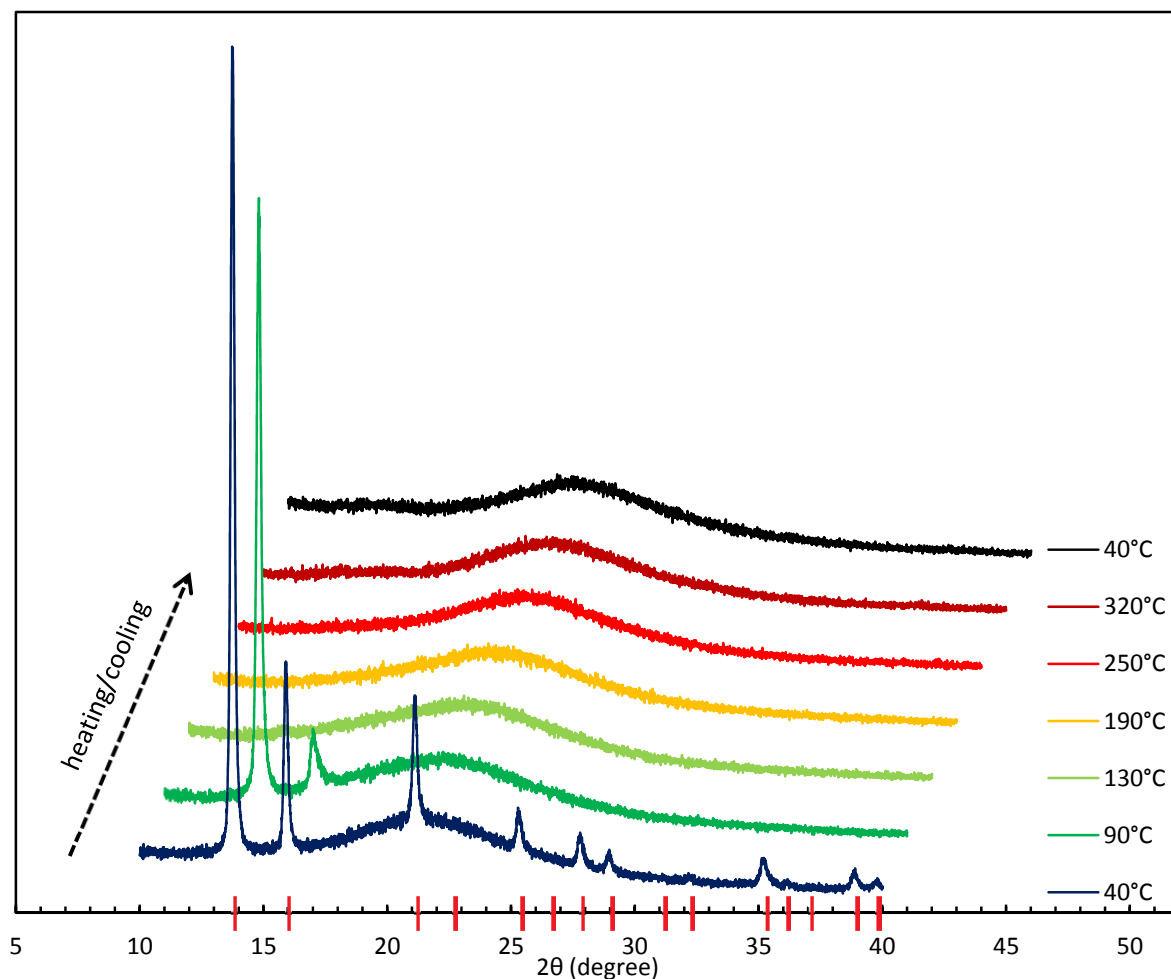


Figure S9. XRD patterns of NScD-treated γ -Mg(BH₄)₂ during heating (held at each temperature for ~2 h, then ramped quickly to the next temperature) and cooling back to near room temperature. The peaks corresponding to γ -Mg(BH₄)₂¹¹ are indicated in red. Each pattern after the initial 40°C pattern is offset by 1 degree in 2 θ from the last.

In an XRD experiment under heating (sample held in a sealed capillary, initially under argon at 1 bar), it was observed that γ -Mg(BH₄)₂ is only stable until ~90°C (see Figure S9). At this temperature, some long range order is maintained as evidenced by the persistence of the low angle peaks. The sample was fully amorphous at 130°C (likely due to pore collapse) and no other phase transitions were observed up to 320°C. Cooling back to 40°C did not result in the crystallization of any phases, indicating that all solid products of decomposition were amorphous.

VII. Nitrogen Adsorption Measurements

Nitrogen adsorption/desorption isotherms of $\gamma\text{-Mg}(\text{BH}_4)_2$ were measured at 77 K using a Micromeritics ASAP 2020 instrument, using default settings for equilibrium determination based on a zeolite standard. Specific surface areas were calculated by the Brunauer-Emmett-Teller (BET) and Langmuir methods over the relative pressure range relevant to each model, respectively. The adsorption isotherms are shown in Figure S10 and the calculated surface areas are shown in Table S1. NScD-treated samples (1x iterated) were found to exhibit an increase in surface area of a factor of ~ 3 due to the removal of guest molecules in the pores. The total surface areas measured were found to be much lower than expected from the crystal structure of $\gamma\text{-Mg}(\text{BH}_4)_2$, but this difference can be attributed to lack of sufficient equilibration at each pressure step in the isotherm. It was reported that very long equilibration times were necessary to achieve equilibrium nitrogen penetration in the pores of $\gamma\text{-Mg}(\text{BH}_4)_2$, requiring experiments up to 5 days in duration.¹¹

Table S1: Surface areas of $\gamma\text{-Mg}(\text{BH}_4)_2$ calculated from N_2 adsorption isotherm measurements.

Material	Density [◊] (g mL^{-1})	BET Surface Area ($\text{m}^2 \text{g}^{-1}$)	BET Fit Range (P/P_0)	Langmuir Surface Area ($\text{m}^2 \text{g}^{-1}$)	Langmuir Fit Range (P/P_0)
Untreated	0.55	58.2 ± 1.9	0.011-0.20	69.0 ± 0.3	0.011-0.77
Untreated	0.55	62.1 ± 1.9	0.010-0.20	71.8 ± 0.5	0.010-0.77
NScD-Treated (1x)	0.55	186.3 ± 9.7	0.009-0.20	217.7 ± 2.3	0.009-0.75

[◊] Indicates density used in SSA calculations, from crystal structure theoretical density¹¹.

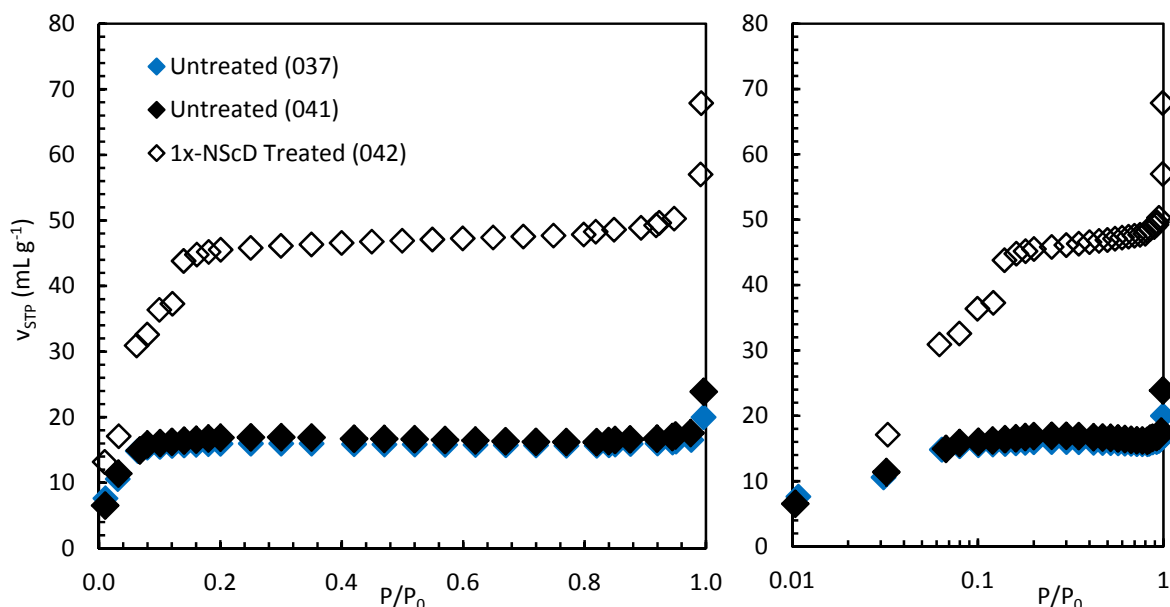


Figure S10. Nitrogen adsorption isotherms of $\gamma\text{-Mg}(\text{BH}_4)_2$ at 77 K: untreated (solid diamonds) and NScD-treated (1x) (empty symbols). Multiple measurements are shown in different colours.

VIII. Attenuated Total Reflectance Infrared Spectroscopy (ATR-IR)

Attenuated total reflectance infrared (ATR-IR) spectra were measured of untreated γ - $\text{Mg}(\text{BH}_4)_2$ (as synthesized), 1x-NScD-treated and 3x-NScD-treated γ - $\text{Mg}(\text{BH}_4)_2$, and commercial $\text{Mg}(\text{BH}_4)_2$ (95%, Sigma Aldrich). The experiments were performed at ambient conditions in inert argon atmosphere using an FTIR spectrometer (Alpha, 4 cm^{-1} resolution, Bruker Corp.) fitted with a diamond ATR accessory. The resulting spectra, averaged over 260 scans each, are shown in Figure S11. The data were normalized based on the absorption band corresponding to the B-H stretching mode of $\text{Mg}(\text{BH}_4)_2$, centered at 2270 cm^{-1} . The notable trend in the identifiable impurity absorption bands are:

1. O-H stretching bands from H_2O were successively reduced by iterated NScD treatments.
2. C-H stretching bands from *n*-butyl impurities were successively reduced by iterated NScD treatments.
3. B-H stretching bands could not be directly attributed to B_2H_6 , and were not substantially affected by NScD treatments except to narrow the dominant peak centered at 2270 cm^{-1} .

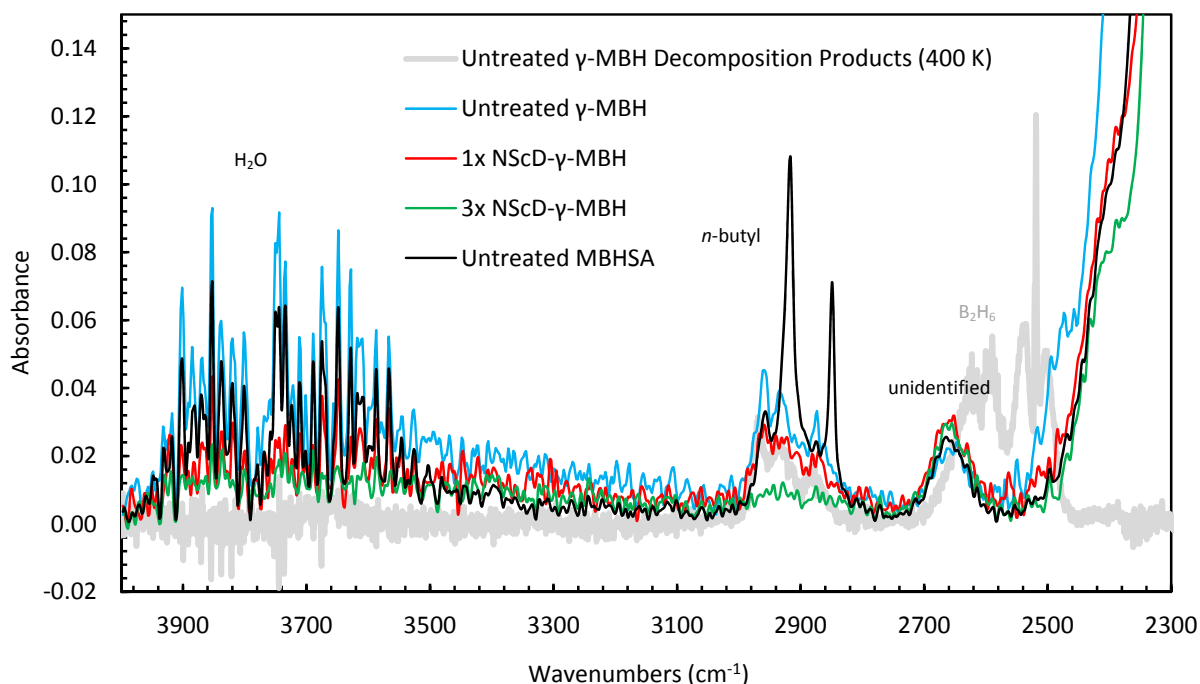


Figure S11. ATR-IR spectra of untreated γ - $\text{Mg}(\text{BH}_4)_2$ (as synthesized), 1x-NScD-treated and 3x-NScD-treated γ - $\text{Mg}(\text{BH}_4)_2$, and commercial $\text{Mg}(\text{BH}_4)_2$ received from Sigma Aldrich (“MBHSA”), showing the O-H and C-H stretching regions (normalized scale). Underlaid is the gas phase absorbance spectrum of the products of decomposition of untreated γ - $\text{Mg}(\text{BH}_4)_2$ at 400 K measured during TPDIR experiments (arbitrarily scaled).

IX. References

1. Li, H. W.; Yan, Y.; Orimo, S.; Züttel, A.; Jensen, C. M. *Energies* **2011**, 4, 185-214.
2. Li, H. W.; Kikuchi, K.; Nakamori, Y.; Ohba, N.; Miwa, K; Towata, S.; Orimo, S. *Acta Mat.* **2008**, 56, 1342-1347.
3. Matsunaga, T.; Buchter, F.; Mauron, P.; Bielman, M.; Nakamori, Y.; Orimo, S.; Ohba, N.; Miwa, K.; Towata, S.; Züttel, A. *J. Alloys Compd.* **2008**, 459, 583-588.
4. Soloveichik, G. L.; Gao, Y.; Rijssenbeek, J.; Andrus, M.; Kniajanski, S.; Bowman, R. C.; Hwang, S. J.; Zhao, J. C. *Int. J. Hydrogen Energ.* **2009**, 34, 916-928.
5. Severa, G.; Rönnebro, E.; Jensen, C.; *Chem. Commun.* **2010**, 46, 421-423.
6. Yan, Y.; Remhof, A; Rentsch, D; Züttel, A. "Hydrogen Desorption of Mg(BH₄)₂: a dodecaborate-free process" *Chem. Commun.* (under review, ID: CC-COM-05-2014-003564)
7. Jeon, E.; Cho, Y. W. *J. Alloys Comp.* **2006**, 422, 273-275.
8. Ravnsbæk, D.; Filinchuk, Y.; Cerenius, Y.; Jakobsen, H. J.; Besenbacher, F.; Skibsted, J.; Jensen, T. R. *Angew. Chem. Int. Ed.* **2009**, 48, 6659-6663
9. Callini, E.; Borgschulte, A.; Ramirez-Cuesta, A. J.; Züttel, A. *Dalton Trans.* **2013**, 42, 719-725.
10. Note: all reported investigations of Mg(BH₄)₂ decomposition products were performed in vacuum conditions.²⁻⁶
11. Filinchuk, Y; Richter, B.; Jensen, T. R.; Dmitriev, V.; Chernyshov, D.; Hagemann, H. *Angew. Chem. Int. Ed.* **2011**, 50, 11162-11166.
12. Borgschulte, A.; Callini, E.; Probst, B.; Jain, A.; Kato, S.; Friedrichs, O.; Remhof, A.; Biemann, M.; Ramirez-Cuesta, A. J.; Züttel, A. *J. Phys. Chem. C* **2011**, 115, 17220-17226.
13. Paskevicius, M.; Pitt, M. P.; Webb, C. J.; Sheppard, D. A.; Filsø, U.; Gray, E. MacA.; Buckley, C. E.; *J. Phys. Chem. C* **2012**, 116, 15231-15240.
14. McHugh, M. A.; Krukonis, V. J. *Supercritical Fluid Extraction*; Butterworth: Stoneham, MA, 1st Ed., **1986**.
15. Hüsing, N.; Schubert, U. *Angew. Chem.* **1998**, 37, 22-45.
16. Cooper, A. I. *J. Mater. Chem.* **2000**, 10, 207-234.
17. Nelson, A. P.; Farha, O. K.; Mulfort, K. L.; Hupp, J. T. *J. Am. Chem. Soc.* **2009**, 131, 458-460.
18. Totten, R. K.; Kim, Y. S.; Weston, M. H.; Farha, O. K.; Hupp, J. T.; Nguyen, S. T. *J. Am. Chem. Soc.* **2013**, 135, 11720-11723.
19. Hugelshofer, C; Borgschulte, A; Callini, E.; Gehrig, J.; Matam, S.; Hog, D. T.; Züttel, A. "The gas-solid reaction of carbon dioxide with alanates" *J. Phys. Chem. C* (submitted May 2014)
20. Giddings, J. C.; Myers, M. N.; McLaren, L.; Keller, R. A. *Science* **1968**, 162, 3849, 67-73.
21. Williams, D. F. *Chem. Eng. Sci.* **1981**, 36, 11, 1769-1788.
22. Moquin, P. H. L.; Temelli, F. *J. Supercrit Fluid* **2008**, 45, 94-101.
23. E. W. Lemmon, M. L. Huber, and M. O. McLinden, 'NIST standard reference database 23: reference fluid thermodynamic and transport properties – REFPROP', Number Version 8.0 in Standard Reference Data Program, **2008**.
24. S.E. Stein, "Infrared Spectra" in NIST Chemistry WebBook, NIST Standard Reference Database Number 69, Eds. P.J. Linstrom and W.G. Mallard, National Institute of Standards and Technology, Gaithersburg MD, 20899, USA, <http://webbook.nist.gov>, (retrieved **2013-2014**).
25. Carpenter, J. D.; Ault, B. S. *J. Phys. Chem.* **1992**, 96, 11, 4288-4294.
26. Wartik, T.; Pearson, R. K. *J. Inorg. Nucl. Chem.* **1958**, 7, 404-411.